

Possibility of Spin-Polarized Electric Current Through Mn-, Fe-, Co-, or Ni-doped
BaSi₂ Predicted by Their Calculated Densities of States.

Yoji Imai¹, Mitsugu Sohma¹, Takashi Suemasu²

¹ *National Institute of Advanced Industrial Science and Technology,*

AIST Tsukuba Central 5, Higashi 1-1 Tsukuba, Ibaraki 305-8565, Japan

² *Institute of Applied Physics, University of Tsukuba,*

1-1-1 Tennohdai, Tsukuba, Ibaraki 305-8573, Japan

Electronic energies and spin-resolved electronic densities-of-states (DOSs) of BaSi₂ whose vacant space is occupied by magnetic elements (Mn, Fe, Co and Ni) are calculated using a first-principle pseudopotential method based on the density-functional theory (DFT) with the generalized gradient approximations. Interstitial compounds of these magnetic elements and BaSi₂ will be energetically possible and interstitial occupancy of BaSi₂ by Fe and, especially, Co atoms will make the materials half-metallic in case the concentration of doped atoms is well controlled.

Key Words: BaSi₂, spintronics, half-metal, interstitial

1. Introduction

Ferromagnetic semiconductors, which are traditional semiconductors doped with transition metals, have been attracting much attention as spintronics materials since the discovery of ferromagnetism in indium arsenide (InAs)¹⁾ or gallium arsenide (GaAs)²⁾ doped with manganese (Mn).

Examples of ferromagnetic semiconductor materials studied thus far include Mn-doped indium antimonide (InSb)³⁾, chromium (Cr)-doped GaN⁴⁾ or AlN⁵⁾, and Mn-, iron (Fe)-, cobalt (Co)-, or Cr-doped indium oxide, zinc oxide, titanium oxide, and tin oxide⁶⁻⁹⁾.

Recently, attentions to the semiconducting silicides such as FeSi₂, BaSi₂ and Mg₂Si are increasing because they are composed of non-toxic and naturally abundant elements in the earth's crust. Among them, BaSi₂, which is promising for solar cell material¹⁰⁾, has a relatively low-dense structure. Therefore, it may accommodate transition metal elements¹. If magnetic elements such as Mn, Fe, Co, or Ni are doped into BaSi₂, it may provide new type of spintronics materials. Controllability of charge carrier (*n*- or *p*-type) of BaSi₂ using 13th and 15th element dopants has been confirmed, which is comparable to the case of oxides where intrinsic defects will cause persistence of conduction type.

We have performed energetic calculations of insertion reactions by Mn, Fe, Co and Ni into BaSi₂ assuming possible insertion sites and clarified the possibility of new type of ferromagnetic semiconductors.

2. Calculation Method

Calculations have been done using CASTEP (Cambridge Serial Total Energy Package) [13], a first-principle pseudopotential method based on the density-functional theory (DFT) [14] for describing the electron–electron interaction, a pseudopotential description of the electron-core interaction, and a plane-wave expansion of the wavefunctions, developed by Payne *et al.*

As for the method of approximation to the exchange-correlation term of the DFT, we used Perdew-Wang Generalized Gradient Approximations (GGA-PW) [15].

The pseudopotential used is the ultrasoft pseudopotential generated by the scheme

¹ In fact, a copper (Cu) atom would be probably inserted into the BaSi₂ lattice. This was inferred from the *n*-type behavior of doped materials [11] and energetic comparison of substitutional and interstitial compounds [12].

of Vanderbilt [16] but is accompanied with the non-linear correction [17, 18] so as to treat the local spin density dependence of the exchange and correlation energy.

Wavefunctions were expanded by plane-waves, the number of plane-wave-expansion of which is characterized by a cutoff energy, E_{cutoff} . The kinetic cutoff energy for the plane-wave expansion of the wavefunctions (E_{cutoff}) was set at 300 eV, corresponding to the Fast Fourier Transformation grid of 45 x 36 x 60 for the calculated unit cell of $\text{Ba}_8\text{Si}_{16}\text{X}_1$ (X: Mn, Fe, Co, or Ni), the details of which will be given later. As for the k -points sampling for the total energy calculation, the Monkhorst-Packe scheme [19] with the mesh parameter of 2 x 3 x 3 was used, which corresponded to the spacing of 0.5 nm^{-1} in the reciprocal space and produced 6 k -points from the irreducible part of the Brillouin zone of $\text{Ba}_8\text{Si}_{16}\text{X}_1$.

Self-consistent iteration convergence was assumed when the total energy difference between successive cycles was less than 0.001eV per atom. Therefore, the numerical values of calculated energy may have errors *ca.* ± 0.025 eV per formula unit at most.

The electronic density states (DOS) curves were obtained by broadening the discrete energy levels using a Gaussian smearing function of 0.07 eV full-width at half-maximum (FWHM) on a grid of k -points generated above. The energies are shifted so that the Fermi energies (E_{Fs}) are aligned with zero.

3. Structures Considered

BaSi_2 belongs to the space group of $Pnma(62)$. In the unit cell of BaSi_2 , there are two crystallographically inequivalent $4c$ sites (Wyckoff notation) for Ba (Ba(1) and Ba(2)), two $4c$ sites for Si (Si(3) and Si(4)) and one $8d$ site for Si (Si(5)). Thus, the unit cell of BaSi_2 contains eight formula units ($\text{Ba}_8\text{Si}_{16}$). It is characterized by isolated Si-tetrahedra separated from each other by more than 1.5 times as large as Si-Si bond distance.

In our previous paper [12], sixteen possible insertion sites per $\text{Ba}_8\text{Si}_{16}$ unit cell were found by using an empty sphere finding algorithm of ESOCS, an augmented spherical wave (ASW) calculation program by Molecular Simulations Inc., and were categorized into four crystallographically inequivalent sites. They are, (1), $4a$ sites; a corner site (0 0 0), xz face-centered site (1/2 0 1/2), y-edge-centered site (0 1/2 0), and a body centered site (1/2 1/2 1/2), (2), $4b$ sites; yz face-centered site (0 1/2 1/2), xy face-centered site (1/2 1/2 0), x-edge-centered site (1/2 0 0), and z-edge-centered site (0 0 1/2), and (3), two $4c$ sites (x 1/4 z), $(-x+1/2 \ 3/4 \ z+1/2)$, $(-x \ 3/4 \ -z)$, and $(x+1/2 \ 1/4 \ -z+1/2)$, where $(x=0.0841, z=0.2749)$ and $(x=$

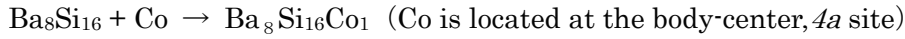
-0.0598, $z = -0.1130$). Those are referred to as $4c(1)$ and $4c(2)$ sites, respectively, hereafter.²

In the present calculations, one of the $4a$, $4b$, $4c(1)$ or $4c(2)$ sites was assumed to be occupied by a guest atom. That is, electronic energies and DOSs of $Ba_8Si_{16}X_1$ (X: Mn, Fe, Co, or Ni) were calculated³. Here, lattice parameters and atomic positions of Ba and Si are assumed to be the same as Schäfer *et al.*'s data for pure $BaSi_2$ [20] and a geometrical optimization has not been performed. Therefore, energetic considerations here are rather tentative. However, we expected that primitive evaluation would be possible so as to judge whether the interstitial compounds assumed here, $Ba_8Si_{16}X_1$, could be realized or not.

4. Results and Discussions

At first, we give the calculated results of formation energy of $Ba_8Si_{16}X_1$ (X=Mn, Fe, Co or Ni) where one X atom is inserted into one of the $4a$, $4b$, $4c(1)$ and $4c(2)$ sites of Ba_8Si_{16} above stated.

In case a Co atom is inserted into the $4a$ sites of Ba_8Si_{16} , the calculated electronic energy of $Ba_8Si_{16}Co_1$ was -8419.929 eV, while those of Ba_8Si_{16} and Co were -7374.810 eV, and -1040.093 eV, respectively. Therefore, energy change for the following insertion reaction, ΔE ,



is $(-8419.929) - ((-7374.810) + (-1040.093)) = -5.026$ eV.

Here, Co in the left side of the chemical reaction equation means an isolated cobalt atom located in the empty lattice of Ba_8Si_{16} .

Similar calculations have been performed for Mn, Fe, Co and Ni for all the possible insertion sites of $4a$, $4b$, $4c(1)$ and $4c(2)$. The results are summarized in Table 1.

² Atomic arrangements around these insertion sites are schematically shown in the previous paper[12]. That is, (1), $4a$ sites are surrounded by four Si atoms composing edges of two Si-tetrahedra: (2), $4b$ sites are located between the two Si atoms which are at the peaks of two Si-tetrahedra: (3), $4c(1)$ sites are surrounded by three Si atoms, one of which is at a peak of one Si-tetrahedron and other two of which are composing an edge of the other Si-tetrahedron: (4), $4c(2)$ sites are surrounded by three Si atoms, which are located at the peaks of three Si-tetrahedra.

³ In concrete, the fractional coordinates of X of the calculated structures of $Ba_8Si_{16}X_1$ are $(1/2 \ 1/2 \ 1/2)$ for the $4a$ site, $(1/2 \ 0 \ 0)$ for the $4b$ site, $(0.5841 \ 1/4 \ 0.2251)$ for the $4c(1)$ site, and $(0.0598 \ 3/4 \ 0.1130)$ for the $4c(2)$ site.

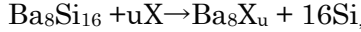
As shown by Table 1, all the insertion reactions have negative energy change. Therefore, $\text{Ba}_8\text{Si}_{16} + \text{X}(\text{atom}) \rightarrow \text{Ba}_8\text{Si}_{16}\text{X}_1$ would proceed spontaneously.

As stated above, this negative energy change does not necessarily mean that interstitial compounds of $\text{Ba}_8\text{Si}_{16}\text{X}_1$ would be formed. Reference states of the present calculations are pure $\text{Ba}_8\text{Si}_{16}$ and an isolated atom of X in the empty unit cell of $\text{Ba}_8\text{Si}_{16}$. Observed cohesive energies of Mn, Fe, Co and Ni are 2.92 eV, 4.28 eV, 4.39 eV, and 4.44 eV, respectively, and the calculated values by GGA-PW previous are 3.73 eV, 4.78 eV, 4.88 eV and 4.52 eV [21]. Though slight overestimations have been experienced by this method, reactions of $\text{Ba}_8\text{Si}_{16} + \text{X}(\text{metal}) \rightarrow \text{Ba}_8\text{Si}_{16}\text{X}_1$ must be possible, since these values of cohesive energy are smaller than the absolute values of the energy change of $\text{Ba}_8\text{Si}_{16} + \text{X}(\text{atom}) \rightarrow \text{Ba}_8\text{Si}_{16}\text{X}_1$ calculated above in most of cases.

Since other competitive reactions such as formation of X-silicides or Ba-X alloy formation, as given by



or



are not considered here, we cannot say that interstitial alloys of BaSi_2 and X will be surely formed. Nevertheless, it might not be unreasonable to expect the formation of interstitial compounds of BaSi_2 and Mn, Fe, Co and Ni.

Figs.1-4 shows the spin resolved DOSs of these interstitial compounds, $\text{Ba}_8\text{Si}_{16}\text{Mn}_1$, $\text{Ba}_8\text{Si}_{16}\text{Fe}_1$, $\text{Ba}_8\text{Si}_{16}\text{Co}_1$, and $\text{Ba}_8\text{Si}_{16}\text{Ni}_1$, respectively, for assumed inserted sites of *4a*, *4b*, *4c(1)* and *4c(2)*.

As for Mn, the most probable insertion site is the *4c(2)* site, followed by the *4b* sites, as shown in Table 1. Calculated magnetic moments of these compounds are 0.0 and $0.20 \mu_B$, respectively, and their spin-resolved DOSs, shown in Figs.1(d) and (b), do not show any distinguishing characteristic to which attention should be paid.

In contrast, Fe-inserted BaSi_2 has a spin-dependent DOSs. Among sites considered, *4a* site-inserted BaSi_2 has the most negative energy, followed by *4c(1)*- and *4b* - site inserted compounds. The spin-resolved DOSs shown in Figs.2(a) and (c) suggests that if *4a* and *4c(1)* sites are occupied, half-metallic character, which means that the spin polarization of electrons is 100% at the Fermi level, would be expected. However, we cannot conclude only *4a* and *4c(1)* sites will be occupied if we take the possible computational error into account since energy difference between the case of occupation of the *4c(1)* sites and that of the *4b* sites is not so large. If *4b* sites are occupied, electronic density of states at its Fermi level is nearly zero for both of

electrons with majority and minority spins, as shown in Fig.2(b), and half-metallicity might not be so remarkable.

Total magnetic moment was calculated to be $2.0 \mu_B$ for both of the $4a$ -sites occupancy and the $4c(1)$ -site occupancy, which is a bit smaller than that of metallic Fe ($2.2 \mu_B$)

This site dependence of the half-metallicity is not the case of Co-inserted BaSi_2 . As shown in Figs.3(a) to (d), all the Co-insertions considered here cause half-metallic spin-dependent DOSs. The most probable insertion sites are $4c(1)$ and $4a$ sites, as in the case of Fe insertion. Total magnetic moments were calculated to be in the range of 0.91 to $0.99 \mu_B$, which is again smaller than metallic Co ($1.7 \mu_B$).

As for Ni insertion, calculated total magnetic moment is zero for all the interstitial occupancy of the sites considered. Their spin-resolved DOSs have no spin direction dependence as shown in Figs.5(a) to (d) and $\text{Ba}_8\text{Si}_{16}\text{Ni}_1$ looks intrinsic semiconductor. This seems strange if we assume Ni atoms will emit their electron to the BaSi_2 lattice. Ni atom seems to neither emit nor absorb electrons to/from the BaSi_2 lattice judging from the present calculations. Electron configuration of Ni atom is considered to be $[\text{Ar}]4s^23d^8$ or $[\text{Ar}]4s^13d^9$ in its atomic state but may be considered as $[\text{Ar}]4s^03d^{10}$ when located in the BaSi_2 lattice.

In the end of the present study, it should be mentioned here that we assumed one atom of Mn to Ni will occupy one of interstitial sites of $\text{Ba}_8\text{Si}_{16}$, unit cell of BaSi_2 , in all the calculations here. Metal concentration doped into the BaSi_2 lattice would be able to be varied to some extent.

As inferred from the shapes of spin-polarized DOSs above mentioned, half-metallicity of $\text{BaSi}_2\text{-Fe(Co)}$ derives from the subtle balance of (1), the degree of spin-polarization dependent on the total magnetic moment of the system, which is determined by the kind and the concentration of doped atoms, and (2), the position of Fermi level which is determined by number of the electrons provided to $\text{Ba}_8\text{Si}_{16}$ by doped atoms. Therefore, half-metallicity of these systems will not be so robust.

We performed calculations so as to confirm the effect of concentration of doped atoms. Examples of calculated DOS where different number of Co atoms are introduced in the $4c(1)$ site of BaSi_2 are shown in Fig.5. Fig.5 (a) shows the spin-polarized DOS of $\text{Ba}_{16}\text{Si}_{32}\text{Co}_1$ where one Co atom is inserted into a $\text{Ba}_{16}\text{Si}_{32}$, which is formed by coalescing two unit cell of $\text{Ba}_8\text{Si}_{16}$. Dilution of Co atoms to double seems not to cause detracting of spin-polarization of carriers, though total magnetic moment per cell is slightly decreased from $0.91 \mu_B/\text{Ba}_8\text{Si}_{16}\text{Co}_1$ to $0.88 \mu_B/\text{Ba}_{16}\text{Si}_{32}\text{Co}_1$.

On the other hand, Fig.5(c) shows the spin-polarized DOS of $\text{Ba}_8\text{Si}_{16}\text{Co}_2$, where

two of four $4c(1)$ sites of $\text{Ba}_8\text{Si}_{16}$ are inserted by Co atoms. Doubling the Co concentration from $\text{Ba}_8\text{Si}_{16}\text{Co}_1$ to $\text{Ba}_8\text{Si}_{16}\text{Co}_2$ will cause shift of Fermi level to lower energy side with respect to the energy gap of DOS for majority-spin electrons and half metallicity will be considerably decreased, though total magnetic moment per cell is increased from $0.91 \mu_B/\text{Ba}_8\text{Si}_{16}\text{Co}_1$ to $1.41 \mu_B/\text{Ba}_8\text{Si}_{16}\text{Co}_2$ ⁴.

Thus, experimental examinations with varied kind and concentration of doped atoms would be necessary so as to optimize the half-metallicity of these systems.

4. Conclusions

We have performed electronic energy and density-of-states (DOS) calculations of BaSi_2 , one of possible sites of interstitial occupancy of which is occupied by magnetic elements (Mn-Ni). It is concluded that BaSi_2 where their vacant site are interstitially occupied by Fe- or Co- may be a half-metal, though further discussions about stability of these alloys compared to other possible phases and those about concentration dependence of the doped elements would be necessary to conclude.

⁴ Magnetic moment per Co atom is slightly decreased, the reason for which has not been understood as of now.

References

- [1] H. Munekata, H. Ohno, S. von Molnár, A. Segmüller, L. L.Chang, L. Esaki, *Phys. Rev. Lett.* **63**, (1989) 1849-1852.
- [2] H. Ohno, A. Shen,, F. Matsukura, A.Oiwa, A. Endo, S.Katsumoto, Y. Iye, *Appl. Phys. Lett.* **69** (1996) 363-365
- [3] V.M. Novotortsev, I.S.Zakharov, A.V. Kochura, S.F.Marenkin, R. Laiho, E. Lahderanta, A. Lashkul, A. G. Veresov, A.V. Molchanov, G. S. Yur'ev, *Russ. J. Inorg Chem.* **51** (2006) 1627-1631
- [4] K. Sato, H. Katayama-Yoshida, *Jpn. J. Appl. Phys* (PART 2) **40** (2001) L485-L487
- [5] S. G. Yang, A. B. Pakhomov, S. T. Hung, C. Y. Wong, *Appl. Phys. Lett.*, **81** (2002) 2418-2420
- [6] K. Ueda, H. Tabata, T. Kawai, *Appl. Phys. Lett.*, **79** (2001) 988-990
- [7] F. Pan, C. Song, X. J. Liu, Y. C. Yang, F. Zeng, *Mater Sci. Eng. Rep.***62** (2008) 1-35
- [8] W. K. Park, R. J. Ortega-Hertogs, J.S. Moodera, A. Punnoose, M. S. Seehra . *J. Appl. Phys.*, **91** (2001) 8093-8095
- [9] A. Punnoose, J. Hays, *J. Appl. Phys.* **97** (2005) Art.No. 10D321
- [10] See, for example, T.Suemasu, K.. Morita, M. Kobayashi, *J. Crystal Growth*, **301** (2007) 680-683
- [11] M. A. Khan, M. Takeishi, Y. Matsumoto, T. Saito, T. Suemasu, *Phys Procedia* **11** (2011)11-14;
See also, M. A. Kahn; T. Saito ;K. Nakamura, M. Baba; W. Du, K.. Toh, K. Toko, T. Suemasu, *Thin Solid Films* **522** (2012) 95-99.
- [12] Y. Imai, A. Watanabe, *Intermetallics* **19** (2011) 1102-1106.
- [13] M.C. Payne, M.P. Teter, D.C. Allan, T.A. Arias, J.D. Joannopoulos, *Rev. Modern Phys.* **64** (1992) 1045.
- [14] W. Kohn, L.J. Sham, *Phys. Rev.* **140** (1965) 1133.
- [15] J. D. Perdew , Y. Wang . *Phys. Rev.* **B 45** (1992) 13244. (←確認PW93)
- [16] D. Vanderbilt, *Phys. Rev.* **B41** (1990) 7892.
- [17]S. G. Louie, S. Froyyen, M. L. Cohen, *Phys. Rev.* **B 26** (1982) 1738.
- [18]F. G. Moroni, G. Kresse, J. Hafner, *Phys. Rev.* **B 56** (1997) 15629.
- [19] H. J. Monkhorst, J. D. Pack , *Phys. Rev.* **B 13** (1976) 5188.
- [20]H. Schäfer, K. H. Janzon, A. Weiss
Angewandte Chem, International Edition, **2** (1963) 393-394
- [21]P. H. T Philipsen, E. J. Baerends : *Phys. Rev.* **B 54** (1996) 5326-5333.

List of Figures and Tables

Fig.1 Interstitial site dependence of spin-resolved total densities of states (DOSs) of $\text{Ba}_8\text{Si}_{16}\text{Mn}_1$.

In this and succeeding figures, the majority (minority)-spin DOS is above (below) the abscissa axis and the total DOS is given per unit cell of $\text{Ba}_8\text{Si}_{16}\text{X}_1$ (X=Mn-Ni).

Fig.2 Interstitial site dependence of spin-resolved total DOSs of $\text{Ba}_8\text{Si}_{16}\text{Fe}_1$.

Please see the text for explanation of *4a*, *4b*, *4c(1)*, and *4c(2)* sites in this and succeeding figures.

Fig.3 Interstitial site dependence of spin-resolved total DOSs of $\text{Ba}_8\text{Si}_{16}\text{Co}_1$.

Fig.4 Interstitial site dependence of spin-resolved total DOSs of $\text{Ba}_8\text{Si}_{16}\text{Ni}_1$. zero.

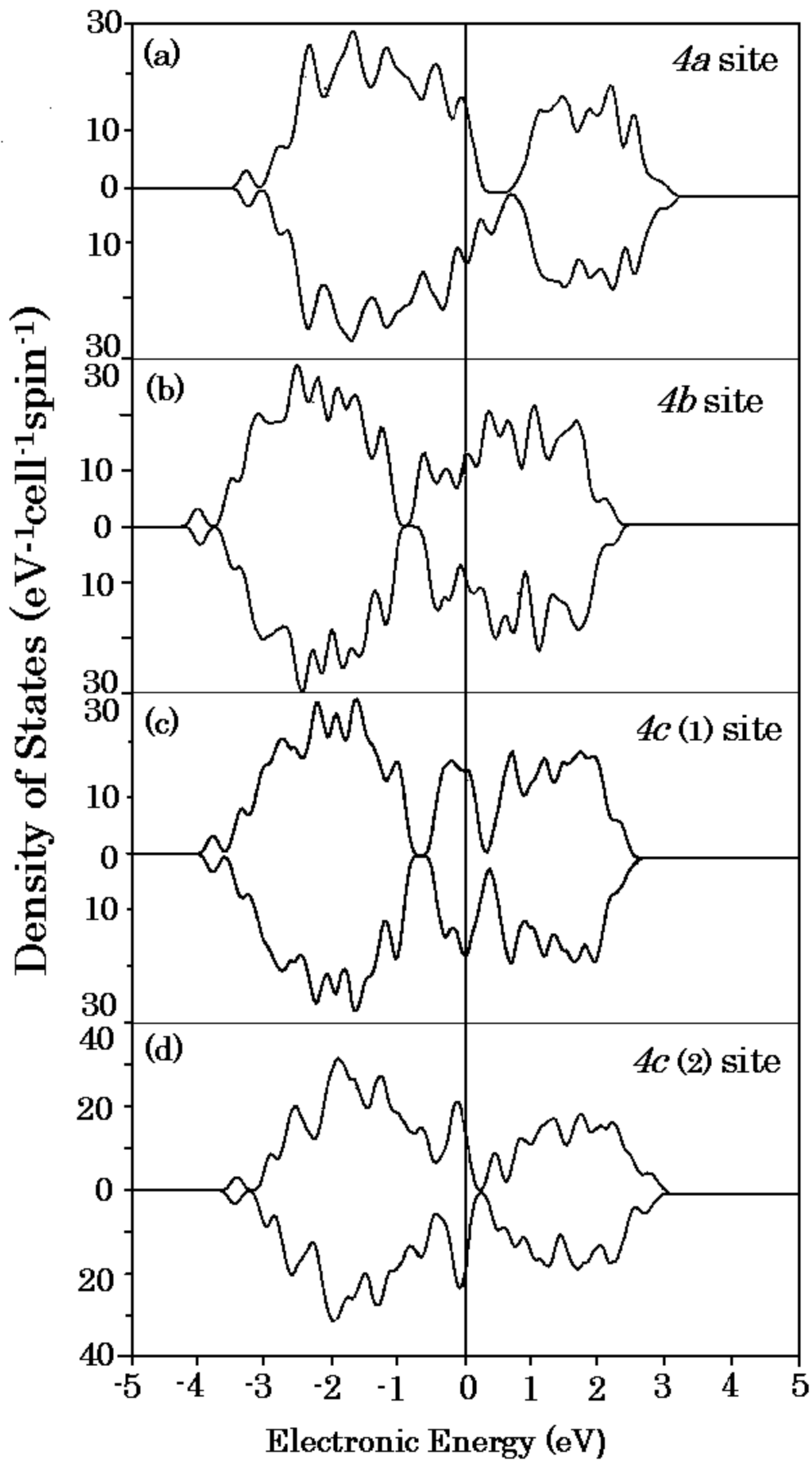
Fig.5 Concentration dependence of spin-resolved total DOSs of $\text{Ba}_8\text{Si}_{16}\text{Co}_x$, (X= 0.5, 1 and 2) where Co atom occupies *4c(1)* sites of $\text{Ba}_8\text{Si}_{16}$.

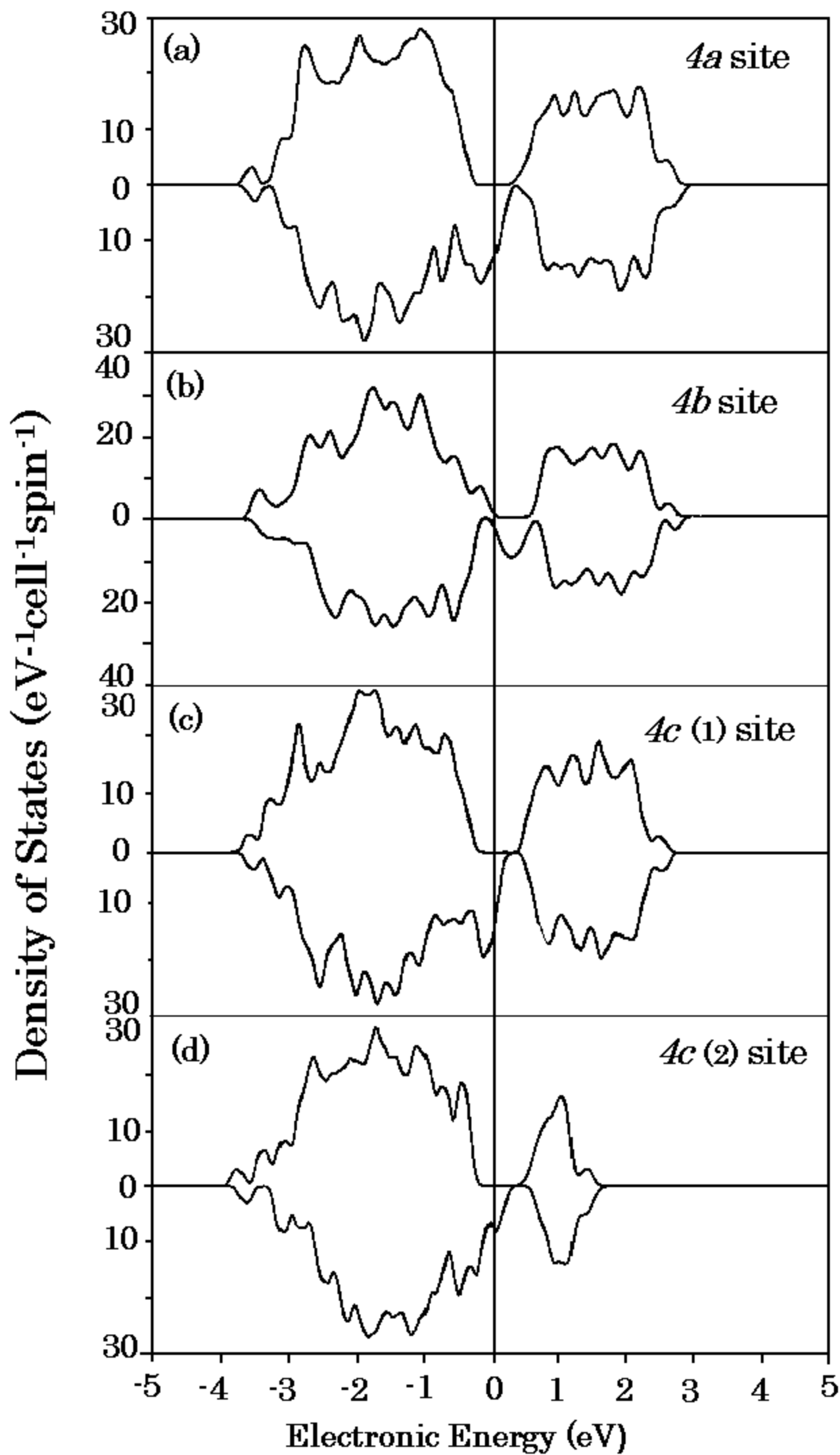
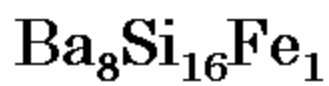
(a), (b) and (c) represent the DOSs of $\text{Ba}_{16}\text{Si}_{32}\text{Co}_1$, $\text{Ba}_8\text{Si}_{16}\text{Co}_1$, and $\text{Ba}_8\text{Si}_{16}\text{Co}_2$, respectively.

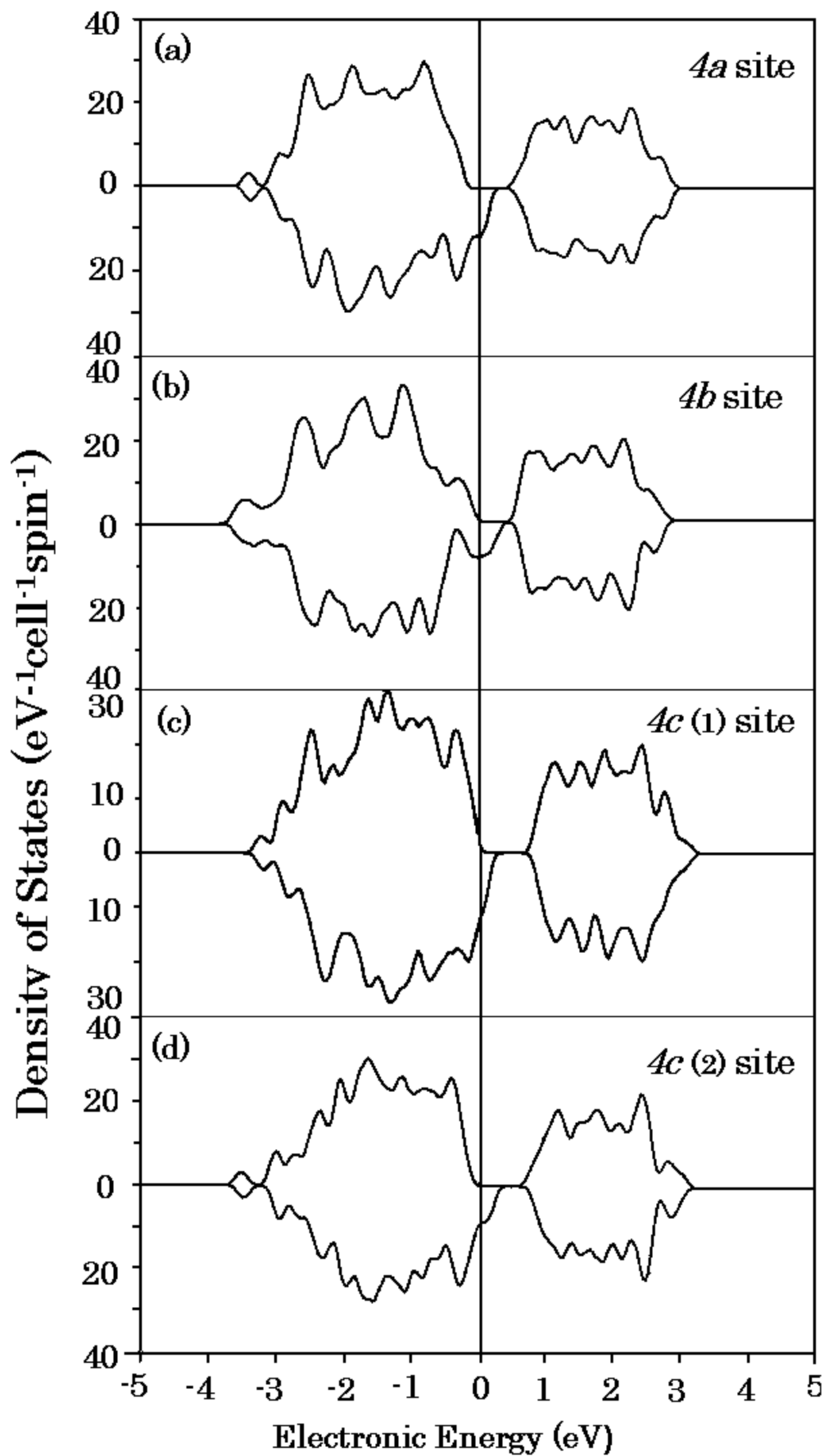
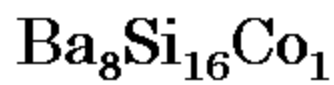
Table1 Interstitial site dependence of calculated energy changes for the reactions

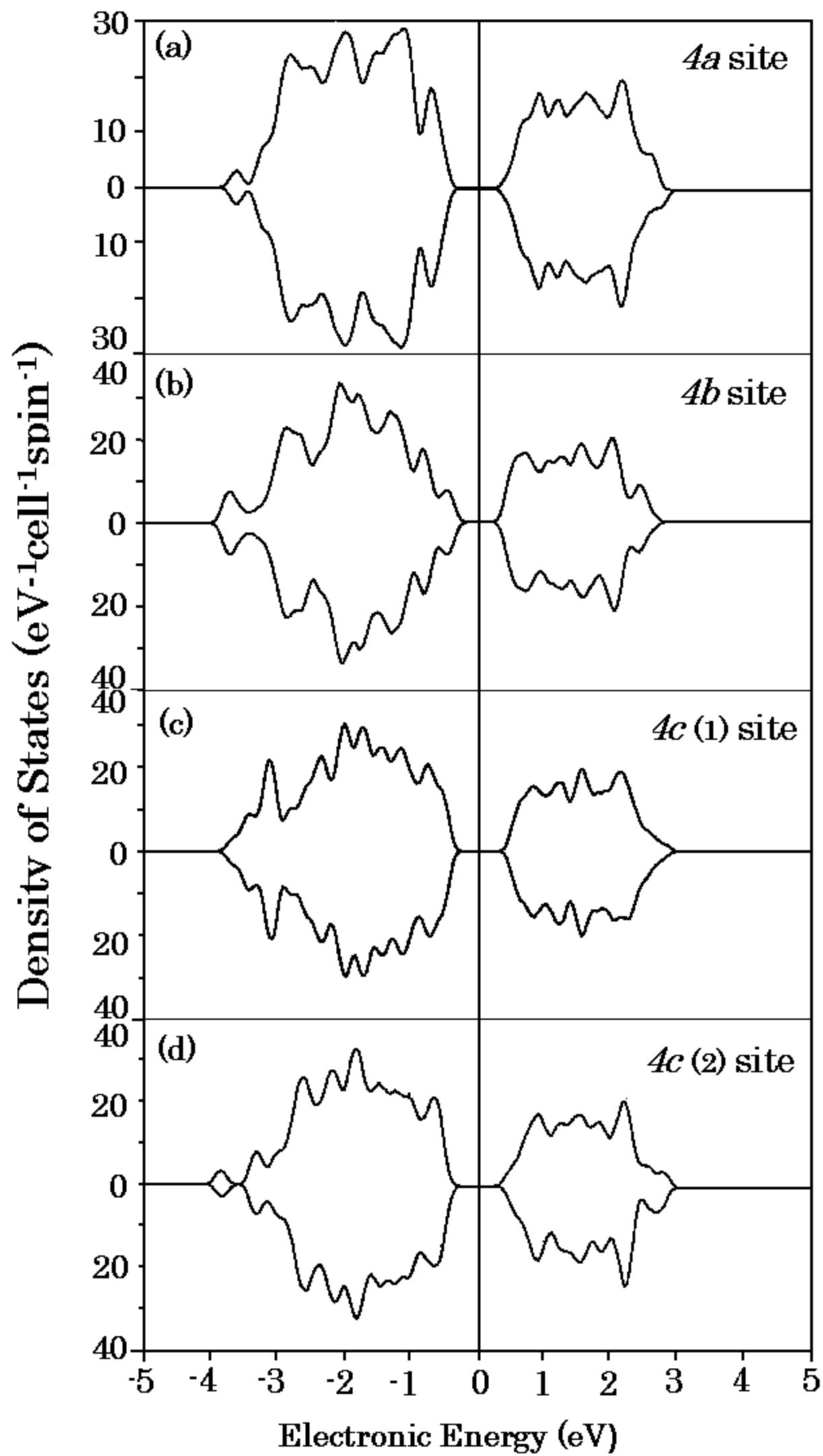
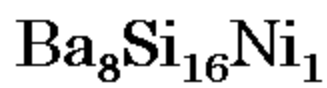


where X is an isolated atom of Mn, Fe, Co, or Ni in the empty lattice of $\text{Ba}_8\text{Si}_{16}$.









4c (1) site

